High-Contrast On/Off Fluorescence Switching via Reversible E–Z Isomerization of Diphenylstilbene Containing the α-Cyanostilbenic Moiety

ARTICLE *in* THE JOURNAL OF PHYSICAL CHEMISTRY C · MAY 2013

Impact Factor: 4.77 · DOI: 10.1021/jp401440s

4 AUTHORS, INCLUDING:

Jong Won Chung
Samsung Advanced Institute of Technology
45 PUBLICATIONS **1,282** CITATIONS
SEE PROFILE

Byeong-Kwan An
Catholic University of Korea
46 PUBLICATIONS **2,796** CITATIONS
SEE PROFILE

THE JOURNAL OF PHYSICAL CHEMISTRY C

Article

pubs.acs.org/JPCC

High-Contrast On/Off Fluorescence Switching via Reversible *E*–*Z* Isomerization of Diphenylstilbene Containing the α-Cyanostilbenic Moiety

Jong Won Chung,[†] Seong-Jun Yoon,[†] Byeong-Kwan An,[‡] and Soo Young Park[†,*]

[†]Center for Supramolecular Optoelectronic Materials and WCU Hybrid Materials Program, Department of Materials Science and Engineering, Seoul National University, Seoul, 151-744 Korea

[‡]Department of Chemistry, The Catholic University of Korea, Bucheon-Si Geyonggi-do, 420-753 Korea

Supporting Information

ABSTRACT: Fluorescence switching or modulation of π-conjugated molecules is of great interest in the area of optoelectronic materials science and technology because of their promising applications. However, the "concentration fluorescence quenching" problems commonly associated with conventional π-conjugated molecules in the solid state were occasionally an obstacle to use of π-conjugated molecules in high-contrast memory storage devices. We designed and synthesized a novel class of fluorescence switching π-conjugated molecule, (*Z*)-CN-MBE, that exhibits a reversible photo/thermal *E*/*Z* isomerization process, accompanied by a remarkable fluorescence on/off switching in the solid state. This may provide a promising way to construct high-contrast optical binary memory storage devices. (*Z*)-CN-MBE is virtually nonfluorescent but exhibits an extraordinary *Z* to *E* isomerization upon external light/thermal stimuli even in the solid state with a concomitant drastic fluorescence enhancement owing to the unique "aggregation-induced enhanced emission" (AIEE)' phenomenon of its trans isomer.

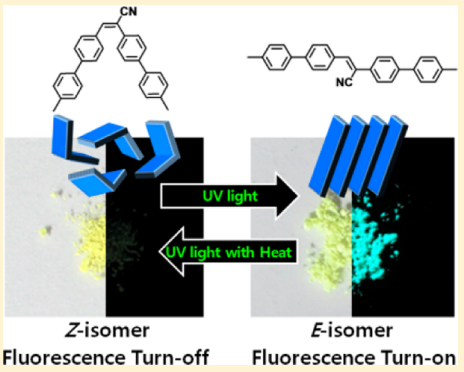

INTRODUCTION

Recently, π-conjugated organic molecules consisting of a (*E*)-α-cyanostilbene unit have rapidly been developed as an attractive molecular platform toward innovative optoelectronics applications, because of their unprecedented photophysical and self-assembling characteristics.[1−7] In particular, (*E*)-2,3-bis(4′-methylbiphenyl-4-ly)acrylonitrile ((*E*)-CN-MBE, Figure 1) is a landmark molecule to this unique class of materials by first demonstrating the concept of 'twist elasticity' in chemical bonds which is responsible for the dramatically enhanced photoluminescence quantum yields (Φ_f) upon *J* aggregation (almost 700-fold increase to give Φ_f = 0.69 in the nanoparticle state).[2a] Such aggregation-induced enhanced emission (AIEE) effect of (*E*)-CN-MBE paved an elegant way to overcoming the well-known "concentration (aggregation) fluorescence quenching" problems commonly associated with conventional π-conjugated molecules in the solid state. Motivated by such extraordinary photophyscial properties of (*E*)-CN-MBE, many different (*E*)-α-cyanostilbene derivatives have been subsequently developed, and their outstanding optical and electrical properties such as AIEE, stimuli-responsive fluorescence modulation,[3−5] high electrical conductivity,[6] and transistor mobility[7] have been extensively investigated for a variety of unique nanostructures self-assembled from them.[2]

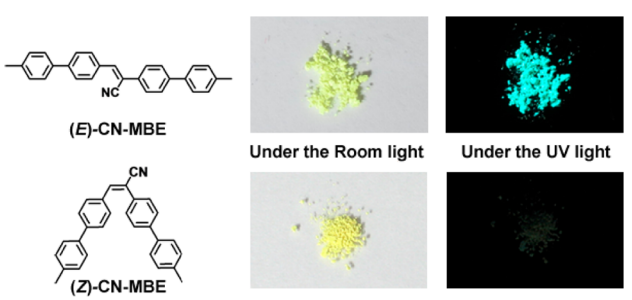

Figure 1. Molecular structure and photoimages of (*E*)- (above) and (*Z*)-CN-MBE (below) under room and UV light.

In spite of such remarkable progress in (*E*)-CN-MBE derivatives so far, (*Z*)-CN-MBE derivatives have seldom been synthesized and investigated for elucidating the fundamental properties of (*Z*)-α-cyanostilbene isomer and also the relevant *E*–*Z* isomerization process. In fact, unlike many ordinary stilbene and azobenzene molecules, very little is known for the *E*–*Z* isomerization process of α-cyanostilbene molecules[8] and especially none for the corresponding fluorescence modulation. The *E*–*Z* isomerization process, if accompanied by concurrent fluorescence switching, may be promising for novel optoelectronic device applications, such as optical memory storage and optical sensor devices, by way of the efficient reversible

Received: February 8, 2013
Revised: April 10, 2013
Published: April 29, 2013

   dx.doi.org/10.1021/jp401440s | *J. Phys. Chem. C* 2013, 117, 11285−11291

Scheme 1. Synthesis of (*Z*)-CN-MBE

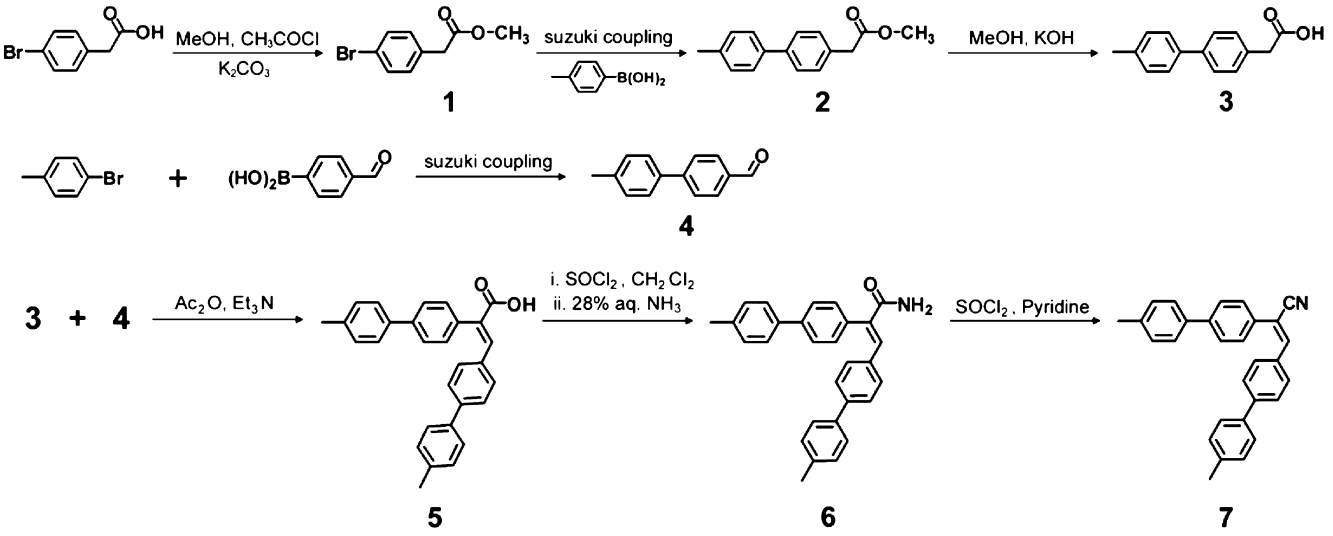

optical modulation through external light or thermal stimuli. In this paper, we report on the remarkable on/off fluorescence switching of CN-MBE implemented via the concerted photo and thermal *E*−*Z* isomerization process.

RESULT AND DISCUSSION

In order to unambiguously interpret the different structural and photophysical properties of the *E* and *Z* isomers, CN-MBE with pure *E* and pure *Z* isomers was separately synthesized (see the Experimental Section). The compositionally pure (*Z*)-CN-MBE was newly synthesized in good yields by Perkin condensation according to the modified procedures of Wei et al.[9] (Scheme 1), while synthesis of pure (*E*)-CN-MBE was simply performed by Knoevenagel reaction as reported earlier by us.[2a] Most distinctly, pure (*E*)- and (*Z*)-CN-MBE (see Figure S1, Supporting Information, for their optimized geometrical structures) were readily distinguished by their fluorescence intensity, i.e., (*E*)-CN-MBE powders showed bright blue fluorescence, while (*Z*)-CN-MBE powders were almost nonfluorescent under 365 nm light illumination (Figure 1). In addition, their isomeric structures could clearly be characterized by ^{1}H NMR spectra (see the Experimental Section), although their mass and elemental compositions are all identical.

The quite different geometry of the π-conjugated backbones significantly affected the absorption and emission properties of (*E*)- and (*Z*)-CN-MBE. The absorption maximum peak (λ_{max}) of (*Z*)-CN-MBE in tetrahydrofuran (THF) solution (2×10^{-5} mol·L^{-1}) was observed at 335 nm with a molar extinction coefficient (ε) of 32 000 cm^{-1}·M^{-1}, whereas (*E*)-CN-MBE showed its absorption λ_{max} at 358 nm with ε = 54 250 cm^{-1}·M^{-1} (Figure 2a). This hypsochromic shift (23 nm) and decrease of molar extinction coefficient (ca. 16 000) of λ_{max} from *E* isomer to *Z* isomer is attributed to the bent structure of the *Z* isomer which generally leads to reduction of the effective conjugation length. This is also supported by the quantum chemical calculation based on time-dependent density functional theory (TD-DFT, B3LYP/6-31G** level implemented with Gaussian 03[10]), which reveals that the absorption λ_{max} and magnitude of oscillator strength (f) at λ_{max} decreases from the *E* form (λ_{max} = 388 nm, f = 1.48) to the *Z* form (λ_{max} = 375 nm, f = 0.70) of CN-MBE.

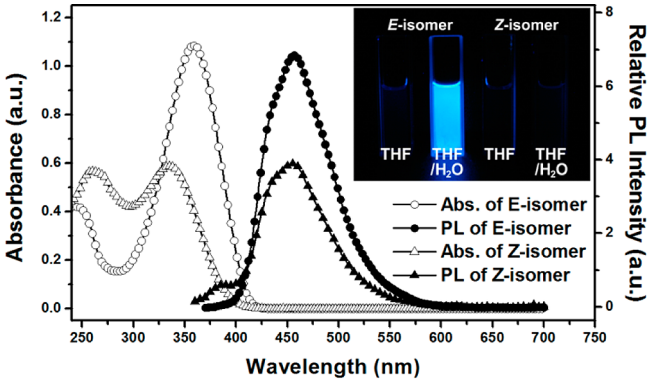

Figure 2. Absorption and PL spectra of (*E*)- and (*Z*)-CN-MBE in solution (in THF, 2×10^{-5} mol·L^{-1}). PL intensity was normalized according to the corresponding UV absorbance. (Inset) Fluorescence image of a solution (in THF, 2×10^{-5} mol·L^{-1}) and nanosuspension (in THF/water (1:9 vol), 2×10^{-5} mol·L^{-1}) of (*E*)- and (*Z*)-CN-MBE, respectively.

As reported previously, the fluorescence emission of (*E*)-CN-MBE was remarkably increased ($^E\Phi_{f,\ solution}$ = 1.0 × 10^{-3} → $^E\Phi_{f,\ nanoparticle}$ = 6.9 × 10^{-1}) with a concurrent bathochromic shift in the emission wavelength ($\lambda_{max,\ solution}$ = 455 nm → $\lambda_{max,\ nanoparticle}$ = 488 nm) upon addition of water into THF solution (forming nanoparticle suspension) due to the synergistic combination of aggregation-induced planarization and specific *J*-type intermolecular stacking[2a] (Figure 2b left, Figure S2, Supporting Information). On the contrary, such AIEE phenomenon was not apparent in (*Z*)-CN-MBE, i.e., no virtual fluorescence emission enhancement via a nanoparticle aggregation process ($^Z\Phi_{f,\ solution}$ = 8.4 × 10^{-4} → $^Z\Phi_{f,\ nanoparticle}$ = 2.0 × 10^{-3}) was observed (Figure 2b right, Figure S2, Supporting Information). This is most likely because the bent-shape structure of (*Z*)-CN-MBE prevents effective molecular planarization and stacking in the aggregation state.

In order to investigate photoisomerization of CN-MBE in solution, the absorption changes of both compositionally pure (*E*)-CN-MBE and (*Z*)-CN-MBE molecules in dilute THF solution (2×10^{-5} mol·L^{-1}) prepared in the dark were monitored under illumination of 365 and 254 nm light (1.2 mW·cm^{-2}) for *E* → *Z* and *Z* → *E* photoisomerization process,

dx.doi.org/10.1021/jp401440s | J. Phys. Chem. C 2013, 117, 11285−11291

respectively. Figure 3 shows that the λ_{max} of all (*E*)-CN-MBE is gradually blue shifted from 358 to 342 nm (photostationary

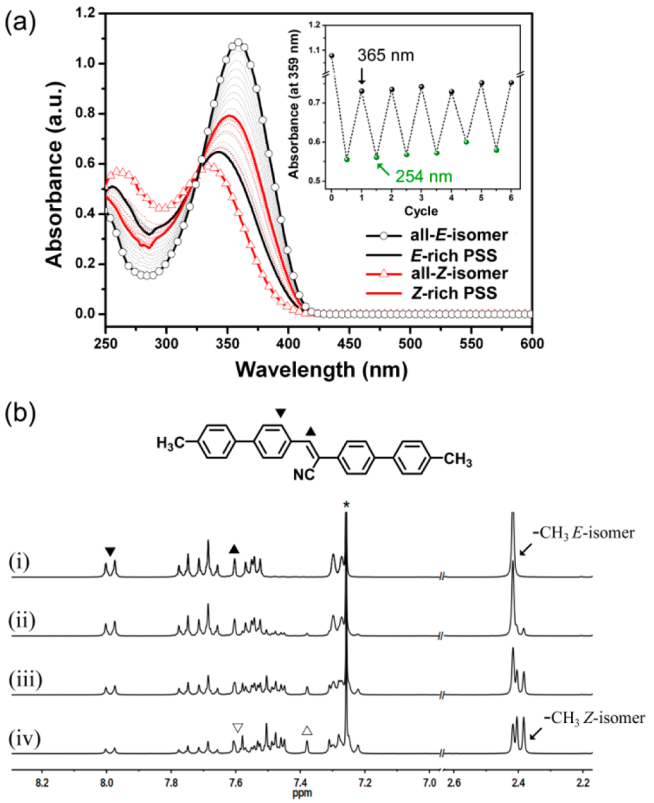

Figure 3. (a) UV−vis absorption spectrum changes of (*E*)- and (*Z*)-CN-MBE in THF (2×10^{-5} mol·L^{-1}) by increasing the illumination time of 365 and 254 nm light (1.2 mW·cm^{-2}), respectively. Black line corresponds to the *E* isomer (circle, initial; solid line, PSS), and red-line represents the *Z* isomer (triangle, initial; solid line, PSS). (Inset) Absorbance at 359 nm of CN-MBE is modulated upon alternative irradiation of 365 (black circle, for 10 min) and 254 nm (green circle, for 2 min) UV light owing to the reversible *E* to *Z* and *Z* to *E* isomerization process. (b) ^{1}H NMR spectrum changes of (*E*)-CN-MBE in $CDCl_3$ upon UV irradiation time of 0 (i), 10 (ii), 60 (iii), and 600 s (iv) (protons in the vinylene and phenyl ring of the *E* form (▲ and ▼) and *Z* form (△ and ▽).

state (PSS), black bold line in Figure 3a) with a decrease of absorbance as a function of exposure time of 365 nm UV light. In addition, the isosbestic point at 326 nm was observed, indicating that two absorbing species (i.e., (*E*)- and (*Z*)-CN-MBE) are present in solution. In contrast, λ_{max} and its absorbance of all (*Z*)-CN-MBE are gradually red shifted and increased until the PSS was reached (red bold line in Figure 3a) upon radiation of 254 nm UV light. It should be noted that the isosbestic point appears at the same position of 326 nm for both cases. These results demonstrate that *E* to *Z* and *Z* to *E* isomerization in solution occurred reversibly between each of the PSS equilibrium upon alternating UV light illumination (see inset image in Figure 3a). On the basis of the conversion equation using absorbance values of *Z* and *E* isomers (see Supporting Information for the equation), it was calculated that the resulting *E*/*Z* conversion ratio of (*E*)- and (*Z*)-CN-MBE is approximately 25/75 ($\lambda_{irra.}$ = 365 nm), and 50/50 ($\lambda_{irra.}$ = 254 nm) at PSS equilibrium, respectively. The photoisomerization process of CN-MBE could also be clearly monitored by ^{1}H NMR spectroscopy because the protons in vinylene and phenyl rings (▲ and ▼ in Figure 3b, respectively) and terminal methyl groups are placed in fairly different configurations.[11] Upon irradiation at 365 nm, the amount of generated *Z* isomer increased gradually with concomitant decrease in the amount of *E* isomer until a PSS was reached. At equilibrium, the *E*/*Z* ratio was determined from the ratio between the terminal methyl proton peak of (*E*)- and (*Z*)-CN-MBE. It was consistent with the conversion ratio obtained using the absorbance values.

For an in-depth understanding of the isomerization process of CN-MBE molecules, the thermal behavior of (*Z*)- and (*E*)-CN-MBE was studied, since the *E* ↔ *Z* isomerization may also be triggered by thermal stimuli. Figure 4 shows the typical

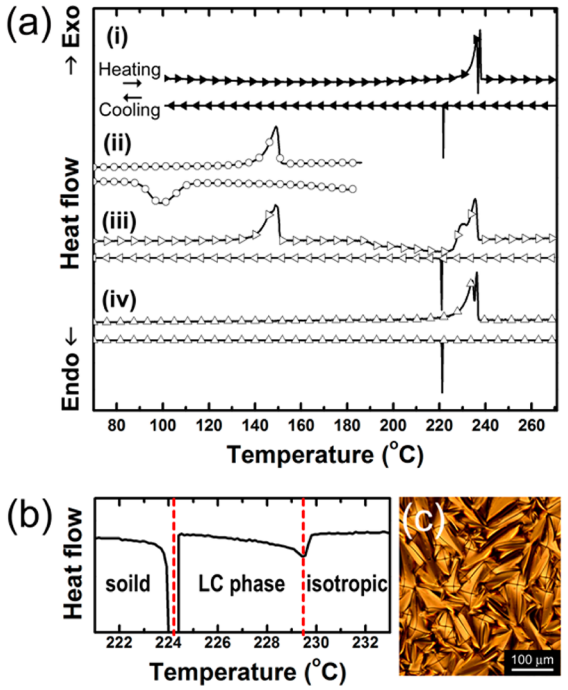

Figure 4. (a) DSC curves of heating and cooling processes for (*E*)- and (*Z*)-CN-MBE. (i) First heating and cooling for (*E*)-CN-MBE. (ii−iv) First to third heating and cooling for (*Z*)-CN-MBE, respectively. (b) Magnitude of the DSC curve in the region, and (c) POM image of Smetic LC phase (224−230 °C) of (*E*)-CN-MBE.

differential scanning calorimetry (DSC) traces of the heating and cooling scans under a heating rate of 1 °C·min^{-1} for both (*E*)- and (*Z*)-CN-MBE. An endothermic transition of (*E*)- and (*Z*)-CN-MBE appeared at 236.0 and 149.1 °C upon the first heating (up to 300 °C for *E*-form (Figure 4i) and 200 °C for the *Z* form (Figure 4ii), indicating the thermal transition of their crystalline melting points. The higher melting point of the *E* isomer than that of the *Z* isomer is quite reasonable, as (*Z*)-CN-MBE may stack with loose packing owing to the bent-shaped structure which consequently leads to weaker $\pi-\pi$ intermolecular interaction. It is interesting to note here that (*E*)-CN-MBE exhibited a Smectic A liquid crystal (LC) phase in the region of 224−230 °C during the first cooling process (Figure 4b), which is confirmed by the appearance of a focal conic fan texture in the polarizing optical microscopy (POM) image (Figure 4c).

In the second heating process (scanning up to 300 °C for both isomers), (*E*)-CN-MBE exhibited the same thermal transition traces of the first heating process but (*Z*)-CN-MBE showed an endothermic transition from around 190 °C

dx.doi.org/10.1021/jp401440s | J. Phys. Chem. C 2013, 117, 11285−11291

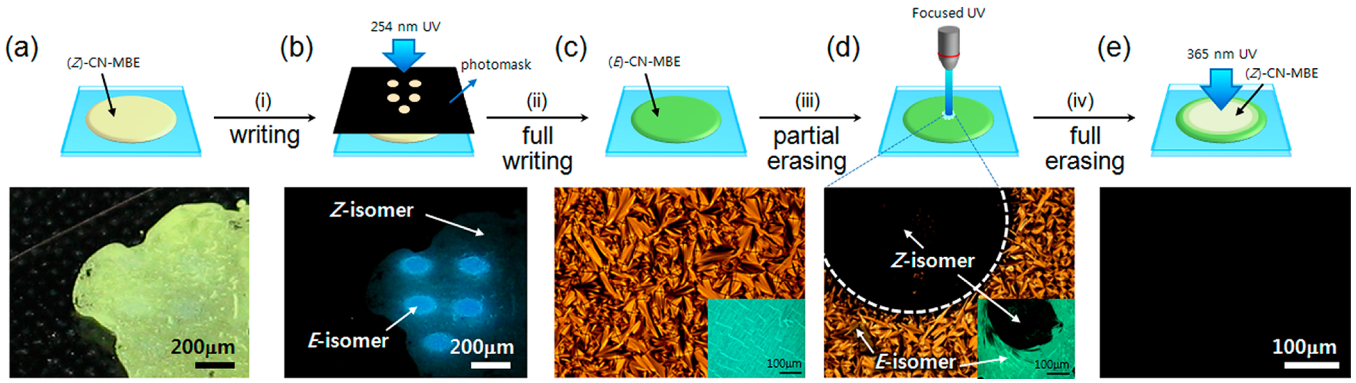

Figure 5. Photo (a–b) and POM image (c–e) changes of (*Z*)-CN-MBE upon UV light irradiation and thermal heating. (a) Initial state: (*Z*)-CN-MBE film in a sandwiched cell under room light. (b) Writing process: (*E*)-CN-MBE (sky-blue emission spot) is generated by (i) 254 nm light irradiation through the photomask. Patterned image is visible under UV light. (c) Full writing process: the remaining part of (*Z*)-CN-MBE is converted into all-(*E*)-CN-MBE by (ii) thermal heating. (d) Partial erasing process: (*Z*)-CN-MBE (dark circle region in white dashed line) is produced by (iii) irradiating with focused UV light at 225 °C. (Inset images of c and d are fluorescence images (scale bar 100 μm), respectively.) (e) Full erasing process: the rest of (*E*)-CN-MBE is converted into all-(*Z*)-CN-MBE by (iv) the same method as in d.

followed by an exothermic transition peak at 235.6 °C (Figure 4iii). This clearly reveals that isomerization from (*Z*)- to (*E*)-CN-MBE occurs by thermal heating. Complete thermal *Z* to *E* isomerization could be verified by the subsequent DSC thermogram (iv) and further confirmed by the ^{1}H NMR spectrum of the thermally treated samples.

The peculiar *E* ↔ *Z* isomerization process of CN-MBE molecules is very useful and attractive for optical memory device applications because this phenomenon may be used to modulate the high-contrast on/off fluorescence switching upon external light and thermal stimuli. In order to realize its full potential in practical optical memory applications, however, an efficient *E* ↔ *Z* photoisomerization process of the CN-MBE molecule is demanded even in the solid state. Therefore, photoisomerization of CN-MBE in the solid state was investigated systematically. First, pure (*E*)-CN-MBE powders were irradiated with 365 nm UV light at room temperature to affect the *E* to *Z* isomerization process up to 1 day, and it was found that no change in ^{1}H NMR spectra was observed before and after light illumination. This result indicates that (*E*)-CN-MBE keeps its molecular conformation even upon long exposure of UV light because (*E*)-CN-MBE molecules are densely packed and confined with strong π–π intermolecular interactions in the solid state which presumably requires a high thermal activation energy for *E* to *Z* isomerization.[12] However, it was found that the *E* to *Z* isomerization process of (*E*)-CN-MBE efficiently occurs in the LC mesophase state (T = 224–230 °C) under UV irradiation ($\lambda_{irra.}$ = 365 nm). Figure S3, Supporting Information, shows that the specific region of the LC phase of (*E*)-CN-MBE is converted to the isotropic phase by irradiating the focused UV light ($\lambda_{irra.}$ = 365 nm), and the fluorescence of this region is quenched after cooling to room temperature. The existence of (*Z*)-CN-MBE was additionally confirmed by ^{1}H NMR spectroscopy.

In contrast to the inefficient *E* to *Z* isomerization process of (*E*)-CN-MBE powder at room temperature, surprisingly, a considerable fluorescent enhancement was detected when (*Z*)-CN-MBE was irradiated under the 254 nm light at room temperature for 10 min (Figure S4, Supporting Information). ^{1}H NMR spectra reveal that the *Z* to *E* isomerization process is successfully developed without any side reaction such as [2 + 2] dimerization and cyclization. This very rare event is probably due to the loose packing induced from bent-shaped molecules which could provide enough volumetric freedom to efficiently trigger the *Z* to *E* isomerization.[13] Most of all, it is worthwhile to point out here that the *Z* to *E* isomerization (even in only 3% conversion) is accompanied by a drastic fluorescence enhancement due to the AIEE effect of (*E*)-CN-MBE (Figure S4a and S4b, Supporting Information) most likely combined with energy transfer between different isomers. This *Z* to *E* isomerization with a concomitant fluorescence enhancement may also occur in other forms of solid states of (*Z*)-CN-MBE such as in an amorphous film or a crystal (Figure S5, Supporting Information). A *Z* to *E* conversion ratio of ~32% was achieved upon irradiation of (*Z*)-CN-MBE in the solid state through continuous irradiation of 254 nm light for 24 h (Figure S6, Supporting Information).

Using a versatile photo/thermal *E* ↔ *Z* isomerization process of CN-MBE molecules we successfully demonstrated the write–erase cycle of the fluorescence optical recording system. Figure 5 shows the operational procedures for recording/erasing fluorescence and POM images in the CN-MBE film. When the (*Z*)-CN-MBE powders in sandwiched glass cells were UV patterned ($\lambda_{irra.}$ = 254 nm) using a photomask, only the UV-irradiated portion was converted to the *E* isomer, leading to turn-on fluorescence change (writing process, Figure 5b). Afterward, the sandwiched glass cell was heated to 236 °C for thermal phase transition from the *Z* to *E* isomer and cooled to room temperature. The fluorescent patterned image was removed because of highly fluorescent background images of all (*E*)-CN-MBE (full-writing process, Figure 5c). Next, the central region of the cell was exposed to the focused 365 nm light with thermal heating at 225 °C (LC phase state) for *E* to *Z* isomerization, which leads to fluorescence quenching of the center region of the cell (partial erasing process, Figure 5d). Finally, the rest of (*E*)-CN-MBE in the fluorescent region of the cell was converted into all nonfluorescent (*Z*)-CN-MBE by the same treatment as the previous process (full erasing process, Figure 5e).

■ CONCLUSION

In summary, a novel class of fluorescence switching π-conjugated molecule, (*Z*)-CN-MBE, was virtually nonfluorescent but exhibited an extraordinary *Z* to *E* isomerization upon external light and thermal stimuli even in the solid state, with a concomitant drastic fluorescence enhancement owing the

unique AIEE phenomenon of its *E* isomer. The highly fluorescent (*E*)-CN-MBE was converted into the nonfluorescent *Z* form via the concerted photo and thermal *E* to *Z* isomerization process, which may provide a promising way to construct high-contrast optical binary memory storage devices.

EXPERIMENTAL SECTION

General Methods. All chemicals were purchased from Aldrich or Lancaster Co. and used without further purification. Synthetic routes and characterization of CN-MBE are described in the Supporting Information. ^{1}H NMR spectra were recorded on DPX Bruker 300 (300 MHz) and Bruker Avance 500 (500 MHz) spectrometers. All NMR spectra were referenced to the solvent. ^{13}C NMR spectra were also measured. Mass spectra were measured using a JEOL JMS AX505WA mass spectrometer. Elemental analysis was carried out using a CE instruments EA110 elemental analyzer. UV−vis absorption spectra were recorded on a Shimadzu UV-1650 PC spectrometer using samples in solutions and nanosuspensions. Fluorescence spectra were recorded on a Shimadzu RF 5301 PC fluorescence spectrometer using samples in solution and the solid state. Compounds of (*E*)- and (*Z*)-CN-MBE were irradiated in the solid state. After irradiation, the powdered sample was dissolved in THF and $CDCl_3$, and spectrophotometric analysis was carried out. Differential scanning calorimetry (DSC) was performed on a Perkin-Elmer DSC7 instrument at a heating and cooling rate of 1 °C min^{-1}. Fluorescence images were obtained using a digital camera (Canon PowerShot G6). Fluorescence and polarized microscopy images were collected on a microscope (Leica). Excitation (365 nm) from an argon ion laser is introduced to the microscope via an optical fiber.

Synthesis of (*E*)-2,3-Bis(4′-methylbiphenyl-4-yl)-acrylonitrile ((*E*)-CN-MBE). This compound was synthesized according to the method described in our previous paper.[2a] ^{1}H NMR (300 MHz, $CDCl_3$, δ): 7.99 (d, J = 9.0 Hz, 2H, aryl H), 7.77 (d, J = 9.0 Hz, 2H, aryl H), 7.69 (t, J = 7.5 Hz, 4H, aryl H), 7.60 (s, 1H, vinyl), 7.56 (d, J = 9.0 Hz, 2H, aryl H), 7.54 (d, J = 9.0 Hz, 2H, aryl H), 7.29 (d, J = 9.0 Hz, 2H, aryl H), 2.42 (s, 6H, methyl). Anal. Calcd for $C_{29}H_{23}N$: C, 90.35; H, 6.01; N, 3.63. Found: C, 90.27; H, 5.94; N, 3.62.

Synthesis of Methyl 2-(4-Bromophenyl)acetate (1). A solution of 2-(4-bromophenyl)acetic acid (7.67 g, 35.67 mmol) in methanol (400 mL) was stirred; acetyl chloride (12.7 mL, 178.34 mmol) was added slowly dropwise at 0 °C. The mixture solution was refluxed for 12 h, and then the reaction mixture was basified with concentrated potassium carbonate with external cooling. The crude mixture was extracted three times with methylene chloride, and the organic fraction was dried with magnesium sulfate. The product was purified by column chromatography on silica gel (*n*-hexane:EtOAc 3:1) to give **1** (yield: 7.97g, 97.7%). ^{1}H NMR (300 MHz, $CDCl_3$, δ): 7.45 (d, J = 8.4 Hz, 2H, aryl H), 7.15 (d, J = 8.5 Hz, 2H, aryl H), 3.69 (s, 3H, methyl H), 3.58 (s, 2H, allyl H). EIMS (m/z (%)): calcd, 229.07; found, 228. Anal. Calcd for $C_9H_9BrO_2$: C, 47.19; H, 3.96; Br, 34.88; O, 13.97. Found: C, 47.48; H, 3.87.

Synthesis of Methyl 2-(4′-Methylbiphenyl-4-yl)-acetate (2). A mixture of **1** (7.97 g, 34.79 mmol), *p*-tolylboronic acid (5.68 g, 41.78 mmol), and tetrakis-(triphenylphosphine) palladium(0) (0.29 g, 0.3 mmol) was dissolved in 120 mL of tetrahydrofuran. After addition of 40 mL of aqueous 2 N potassium carbonate solution, the reaction mixture was stirred at 85 °C and refluxed for 1 day. The cooled crude mixture was poured into 500 mL of water and extracted with ethyl acetate (400 mL) and then dried over anhydrous magnesium sulfate. Finally, silica gel column chromatography (*n*-hexane:EtOAc 3:1) gave the product as a white powder (7.0 g, 29.13 mmol) in 83.7% yield. ^{1}H NMR (300 MHz, $CDCl_3$, δ): 7.53 (d, J = 8.3 Hz, 2H, aryl H), 7.47 (d, J = 8.2 Hz, 2H, aryl H), 7.33 (d, J = 8.2 Hz, 2H, aryl H), 7.24 (d, J = 8.5 Hz, 2H, aryl H), 3.71 (s, 3H, methoxy H), 3.66 (S, 2H, allyl H), 2.39 (s, 3H, methyl). EIMS (m/z (%)): calcd, 240.30; found, 240. Anal. Calcd for $C_{16}H_{16}O_2$: C, 79.97; H, 6.71; O, 13.32. Found: C, 79.67; H, 6.24.

Synthesis of 2-(4′-Methylbiphenyl-4-yl)acetic Acid (3). Compound **2** (6.9 g, 28.71 mmol) was dissolved in methanol (500 mL) at room temperature, and potassium hydroxide (11.5 g, 287.14 mmol) was added dropwise. The reaction mixture was stirred and refluxed overnight. The mixture was extracted with ethyl acetate and water, and HCl was added until pH 2. The product was extracted with ethyl acetate, the organic layer was dried with magnesium sulfate, and then the solvent was evaporated three times to give the product (6.15g, 27.13 mmol) in 91.9% yield. ^{1}H NMR (300 MHz, $CDCl_3$, δ): 7.54 (d, J = 8.3 Hz, 2H, aryl H), 7.47(d, J = 8.2 Hz, 2H, aryl H), 7.34(d, J = 8.2 Hz, 2H, aryl H), 7.24(d, J = 8.5 Hz, 2H, aryl H), 3.69(s, 2H, allyl H), 2.39(s, 3H, methyl H). EIMS (m/z (%)): calcd, 226.27; found, 226. Anal. Calcd for $C_{15}H_{14}O_2$: C, 79.62; H, 6.24; O, 14.14. Found: C, 79.84; H, 6.01.

Synthesis of 4′-Methylbiphenyl-4-carbaldehyde (4). 1-Bromo-4-methylbenzene (6.63 g, 38.76 mmol) was reacted with 4-formylphenylboronic acid (6.39 g, 42.64 mmol) according to the procedure described in our previous literature.[2a] A white powder was obtained in 78.2% yield.

Synthesis of (*Z*)-2,3-Bis(4′-methylbiphenyl-4-ly)acrylic Acid (5). A mixture of **3** (6.0 g, 26.47 mmol), **4** (6.23 g, 31.76 mmol), and triethylamine (4.43 mL, 31.76 mmol) in acetic anhydride (50 mL) was refluxed with stirring under argon for 1 h. Water (80 mL) was added to the reaction mixture, and the temperature was maintained at 90−100 °C during addition. The reaction mixture was cooled to room temperature, and the solid was collected by filtration and recrystallization from ethanol. A yellow powder was obtained in 59.9% yield. ^{1}H NMR (300 MHz, $CDCl_3$, δ): 7.72 (s, 1H, vinyl H), 7.59 (m, J = 13.1 Hz, 8H, aryl H), 7.48 (d, J = 8.1 Hz, 4H, aryl H), 7.26 (d, J = 7.9 Hz, 4H, aryl H), 2.16 (s, 6H, methyl H). EIMS (m/z (%)): calcd, 404.50; found, 404. Anal. Calcd for $C_{29}H_{24}O_2$: C, 86.11; H, 5.98; O, 7.91. Found: C, 86.74; H, 5.62.

Synthesis of (*Z*)-2,3-Bis(4′-methylbiphenyl-4-ly)-acrylamide (6). To a solution of **5** (4.0 g, 9.89 mmol) in dichloromethane (200 mL) was slowly added thionyl chloride (25 mL) in dimethylformamide (5 mL). The reaction mixture was stirred for 1 h at room temperature and concentrated in vacuo. To a solution of the reaction residue in dichloromethane (40 mL) was carefully added 28% ammonium hydroxide aqueous solution (4 mL). The reaction mixture was stirred for 1 h at room temperature. The reaction mixture was diluted with distilled water (100 mL) and extracted with dichloromethane (100 mL, × 2). The combined organic layers were washed with brine, dried over magnesium sulfate, and concentrated to dryness. The resulting residue was purified by flash column chromatography on silica gel (*n*-hexane/EtOAc, 1:1) to give acrylamide **6** (2.96 g, 7.34 mmol) as a white solid in 74.2%. ^{1}H NMR (300 MHz, $CDCl_3$, δ): 7.93 (s, 1H, vinyl H), 7.73 (d, J = 8.3 Hz, 2H, aryl H), 7.56 (d, J = 8.1 Hz, 2H, aryl H), 7.42 (d, J = 8.3 Hz, 2H, aryl H), 7.39 (m, J = 8.4 Hz, 4H, aryl H), 7.29 (d,

J = 7.9 Hz, 2H, aryl H), 7.20 (d, J = 7.9 Hz, 2H, aryl H), 7.13 (d, J = 8.3 Hz, 2H, aryl H), 2.42 (s, 3H, methyl H), 2.36 (s, 3H, methyl H). EIMS (m/z (%)): calcd, 403.51; found, 403. Anal. Calcd for $C_{29}H_{25}NO$: C, 86.32; H, 6.24; N, 3.47; O, 3.97. Found: C, 86.52; H, 5.96.

Synthesis of (*Z*)-2,3-Bis(4′-methylbiphenyl-4-ly)-acrylonitrile (7) ((*Z*)-CN-MBE). To solution of **6** (2.96 g, 7.34 mmol) in pyridine (100 mL) was slowly added thionyl chloride (27 mL). The reaction mixture was stirred for 6 h at room temperature and then concentrated in vacuo. The resulting residue was purified by flash column chromatography on silica gel (*n*-hexane:EtOAc 1:1) to give the product as a yellow green powder (0.95 g, 2.46 mmol) in 33.6% yield. ^{1}H NMR (300 MHz, $CDCl_3$, δ): δ 7.59 (d, J = 8.1 Hz, 2H, aryl H), 7.52 (d, J = 8.1 Hz, 4H, aryl H), 7.47 (m, J = 8.3 Hz, 4H, aryl H), 7.38 (s, 1H, vinyl H), 7.30 (d, J = 8.7 Hz, 4H, aryl H), 7.24 (d, J = 8.4 Hz, 2H, aryl H), 2.41 (s, 3H, methyl H), 2.38 (s, 3H, methyl H). ^{13}C NMR (125 MHz, $CDCl_3$, δ): 113.89, 120.54, 127.01, 127.09, 127.65, 129.54, 129.85, 130.55, 131.61, 132.51, 137.24, 138.05, 142.22, 142.75, 143.80. EIMS (m/z (%)): calcd, 385.50; found, 385. Anal. Calcd for $C_{29}H_{23}N$: C, 90.35; H, 6.01; N, 3.63. Found: C, 90.37; H, 6.02; N, 3.63.

■ ASSOCIATED CONTENT

Supporting Information

Optimized geometrical structure of the cis and trans isomer, UV−vis spectrum, and optical microscope images. This material is available free of charge via the Internet at http://pubs.acs.org.

■ AUTHOR INFORMATION

Corresponding Author

*E-mail: parksy@snu.ac.kr.

Notes

The authors declare no competing financial interest.

■ ACKNOWLEDGMENTS

This work was supported by the Basic Science Research Program through the National Research Foundation of Korea (NRF) funded by the Ministry of Education, Science, and Technology (CRI; RIAMIAM0209(0417-20090011)).

■ REFERENCES

(1) (a) Zhan, X.; Wang, S.; Liu, Y.; Wu, X.; Zhu, D. New Series of Blue-Emitting and Electron-Transporting Copolymers Based on Cyanostilbene. *Chem. Mater.* **2003**, *15*, 1963−1969. (b) Zhu, L.-L.; Li, X.; Ji, F.-Y.; Ma, X.; Wang, Q.-C.; Tian, H. Photolockable Ratiometric Viscosity Sensitivity of Cyclodextrin Polypseudorotaxane with Light-Active Rotor Graft. *Langmuir* **2009**, *25*, 3482−3486. (c) Dou, C.; Han, L.; Zhao, S.; Zhang, H.; Wang, Y. Multi-Stimuli-Responsive Fluorescence Switching of a Donor−Acceptor π-Conjugated Compound. *J. Phys. Chem. Lett.* **2011**, *2*, 666−670.

(2) (a) An, B.-K.; Kwon, S. K.; Jung, S. D.; Park, S. Y. Enhanced Emission and Its Switching in Fluorescent Organic Nanoparticles. *J. Am. Chem. Soc.* **2002**, *124*, 14410−14415. (b) An, B.-K.; Lee, D. S.; Lee, J. S.; Park, Y. S.; Song, H. S.; Park, S. Y. Strongly Fluorescent Organogel System Comprising Fibrillar Self-Assembly of a Trifluoromethyl-Based Cyanostilbene Derivative. *J. Am. Chem. Soc.* **2004**, *126*, 10232−10233. (c) An, B.-K.; Gihm, S. H.; Chung, J. W.; Park, C. R.; Kwon, S. K.; Park, S. Y. Color-Tuned Highly Fluorescent Organic Nanowires/Nanofabrics: Easy Massive Fabrication and Molecular Structural Origin. *J. Am. Chem. Soc.* **2009**, *131*, 3950−3957. (d) An, B.-K.; Gierschner, J.; Park, S. Y. π-Conjugated Cyanostilbene Derivatives: A Unique Self-Assembly Motif for Molecular Nanostructures with Enhanced Emission and Transport. *Acc. Chem. Res.* **2012**, *45*, 544−554.

(3) (a) Chung, J. W.; Yoon, S. J.; Lim, S. J.; An, B. K.; Park, S. Y. Dual-mode switching in highly fluorescent organogels: binary logic gates with optical/thermal inputs. *Angew.Chem., Int. Ed.* **2009**, *48*, 7030−7034. (b) Lim, S. J.; An, B. K.; Jung, S. D.; Chung, M. A.; Park, S. Y. Photoswitchable Organic Nanoparticles and a Polymer Film Employing Multifunctional Molecules with Enhanced Fluorescence Emission and Bistable Photochromism. *Angew. Chem., Int. Ed.* **2004**, *43*, 6346−6350. (c) Lim, S. J.; An, B. K.; Park, S. Y. Bistable Photoswitching in the Film of Fluorescent Photochromic Polymer: Enhanced Fluorescence Emission and Its High Contrast Switching. *Macromolecules* **2005**, *38*, 6236−6239.

(4) (a) Chung, J. W.; An, B. K.; Park, S. Y. A Thermoreversible and Proton-Induced Gel−Sol Phase Transition with Remarkable Fluorescence Variation. *Chem. Mater.* **2008**, *20*, 6750−6755. (b) An, B. K.; Kwon, S. K.; Park, S. Y. Highly Sensitive Fluorescence Probes for Organic Vapors: On/off and Dual Color Fluorescence Switching. *Bull. Korean Chem. Soc.* **2005**, *26*, 1555−1559.

(5) (a) Chung, J. W.; You, Y.; Huh, H. S.; An, B. K.; Yoon, S. J.; Kim, S. H.; Lee, S. W.; Park, S. Y. Shear- and UV-Induced Fluorescence Switching in Stilbenic π-Dimer Crystals Powered by Reversible [2 + 2] Cycloaddition. *J. Am. Chem. Soc.* **2009**, *131*, 8163−8172. (b) Yoon, S.-J.; Chung, J. W.; Gierschner, J.; Kim, K. S.; Choi, M.-G.; Kim, D.; Park, S. Y. Multistimuli Two-Color Luminescence Switching via Different Slip-Stacking of Highly Fluorescent Molecular Sheets. *J. Am. Chem. Soc.* **2010**, *132*, 13675−13683.

(6) (a) Kim, J. H.; Jung, Y.; Chung, J. W.; An, B.-K.; Park, S. Y. Fabrication of a Patterned Assembly of Semiconducting Organic Nanowires. *Small* **2009**, *5*, 804−807. (b) Chung, J. W.; An, B.-K.; Hirato, F.; Kim, J. H.; Jinnai, H.; Park, S. Y. Selected-Area In Situ Generation of Highly Fluorescent Organic Nanowires Embedded in a Polymer Film: The Solvent-Vapor-Induced Self-Assembly Process. *J. Mater. Chem.* **2010**, *20*, 7715−7720. (c) Kim, J. H.; Watanabe, A.; Chung, J. W.; Jung, Y.; An, B.-K.; Tada, H.; Park, S. Y. All-Organic Coaxial Nanocables with Interfacial Charge-Transfer Layers: Electrical Conductivity and Light-Emitting-Transistor Behavior. *J. Mater. Chem.* **2010**, *20*, 1062−1064.

(7) Yun, S. W.; Kim, J. H.; Shin, S.; Yang, H.; An, B.-K.; Yang, L.; Park, S. Y. High-Performance n-type Organic Semiconductors: Incorporating Specific Electron-Withdrawing Motifs to Achieve Tight Molecular Stacking and Optimized Energy Levels. *Adv. Mater.* **2012**, *24*, 911−915.

(8) (a) Gulino, A.; Lupo, F.; Condorelli, G. G.; Fragala, M. E.; Amato, M. E.; Scarlata, G. Reversible Photoswitching of Stimuli-Responsive Si(100) Surfaces Engineered with an Assembled 1-Cyano-1-Phenyl-2-[4′-(10-Undecenyloxy)Phenyl]-Ethylene Monolayer. *J. Mater. Chem.* **2008**, *18*, 5011−5018. (b) Zhu, L.; Ang, C. Y.; Li, X.; Nguyen, K. T.; Agren, H.; Zhao, Y. Luminescent Color Conversion on Cyanostilbene-Functionalized Quantum Dots Via In-Situ Photo-Tuning. *Adv. Mater.* **2012**, *24*, 4020−4024.

(9) Wei, L. Y.; Brossi, A.; Kendall, R.; Bastow, K. F.; Morris-Natschke, S. L.; Shi, Q.; Lee, K. H. Antitumor Agents 251: Synthesis, Cytotoxic Evaluation, and Structure-Activity Relationship Studies of Phenanthrene-Based Tylophorine Derivatives (PBTs) as a New Class of Antitumor Agents. *Bioorg. Med. Chem.* **2006**, *14*, 6560−6569.

(10) Frisch, M. J.; et al. *Gaussian 03*; Gaussian, Inc.: Wallingford CT, 2004.

(11) (a) Bottino, F. A.; Scarlata, G.; Sciotto, D.; Torre, M. A. Simple ^{1}H NMR Approach to the Conformations of α,β-Diarylacrylonitriles. *Tetrahedron* **1982**, *38*, 3713−3719. (b) Alberghina, G.; Amato, M. E.; Fisichella, S.; Pisano, D. Side-Chain Nucleophilic Reactivity of Five-Membered Heterocyclic Rings: Base-Catalysed Reactions of Aldehydes with Phenylacetonitrile. *J. Chem. Soc., Perkin Trans.* **1988**, *2*, 295−298.

(12) (a) Natarajan, A.; Mague, J. T.; Venkatesan, K.; Arai, T.; Ramamurthy, V. Volume-Demanding Cis−Trans Isomerization of 1,2-Diaryl Olefins in the Solid State. *J. Org. Chem.* **2006**, *71*, 1055−1059. (b) Fengqiang, Z.; Motoyoshiya, J.; Nishii, Y.; Aoyama, H.; Kakehi, A.; Shiro, M. Different Photochemical Behavior of Bis(biphenyl)ethylenes

and Ethenes in Solution and in the Solid-State: Structurally Controlled Z/E-Photoisomerization in the Solid-State. *J. Photochem. Photobiol. A Chem.* **2006**, *184*, 44−49.

(13) (a) Uda, M.; Mizutani, T.; Hayakawa, J.; Momotake, A.; Ikegami, M.; Nagahata, R.; Arai, T. Photoisomerization of Stilbene Dendrimers: The Need for a Volume-conserving Isomerization Mechanism. *Photochem. Photobiol.* **2002**, *76*, 596−605. (b) Tanaka, K.; Hiratsuka, T.; Ohba, S.; Naimi-Jamal, M. R.; Kaupp, G. Unidirectional Cis−Trans Photoisomerization of Cis-3,30-Bis-(diphenylhydroxymethyl)stilbene in Inclusion Complex Crystals. *J. Phys. Org. Chem.* **2003**, *16*, 905−912.